

Dynamic magnetic reconnection in three space dimensions: Fan current solutions

I. J. D. Craig^{a)} and R. B. Fabling

Department of Mathematics, University of Waikato, Private Bag 3105 Hamilton, New Zealand

(Received 5 September 1997; accepted 1 December 1997)

The problem of incompressible, nonlinear magnetic reconnection in three-dimensional “open” geometries is considered. An analytic treatment shows that dynamic “fan current” reconnection may be driven by superposing long wavelength, finite amplitude, plane wave disturbances onto three-dimensional magnetic X -points. The nonlinear reconnection of the field is preceded by an advection phase in which magnetic shear waves drive large currents as they localize in the vicinity of the magnetic null. Analytic arguments, reinforced by detailed simulations, show that the ohmic dissipation rate can be independent of the plasma resistivity if the merging is suitably driven.

© 1998 American Institute of Physics. [S1070-664X(98)01703-0]

I. INTRODUCTION

The physical importance of magnetic reconnection is well recognized. Reconnection is the only mechanism that allows a highly conducting plasma to simplify its magnetic-field topology (e.g., Parker¹). That is, by cutting and rejoining magnetic-field lines at null points in the field, magnetic energy can be released to the fluid, either as plasma heating or as the kinetic energy of mass motion. Yet, for reconnection to yield a significant energy release rate in a weakly resistive plasma, strong current densities must develop over very small length scales. It is this fact—when coupled with the intrinsic difficulty of handling the nonlinear magnetohydrodynamic equations—that complicates the development of plausible magnetic reconnection mechanisms.

In the past, numerical simulations have provided the primary tool for investigating dynamic models of reconnection (e.g., Biskamp²). Although simulations provide much insight into the problem, they are generally limited to phenomenological investigations at high plasma resistivities, orders of magnitude beyond what is physically realistic. There are also difficulties with the boundary conditions—especially for classical, steady-state merging, in open geometries—that lead to notorious problems of interpretation.³

It has recently become clear however, that analytic progress can be made with the classical, incompressible reconnection problem. Craig and Henton⁴ first demonstrated that the planar, steady-state problem yields an exact reconnection “shear flow” solution, expressible in terms of named functions. This analysis generalizes naturally to viscous solutions,⁵ and time-dependent, planar models.⁶ But of more interest in the present context is the extension to three space dimensions.⁷ Here there are two types of solutions—namely fan and spine models to use the nomenclature of Priest and Titov⁸—depending on whether the reconnection involves classical current sheets or quasi-cylindrical tubes. The spine model provides extremely rich, tubular current

structures, but it seems doubtful whether these can contain sufficient magnetic energy for many applications—for instance, for explaining the huge, explosive release of the solar flare.⁹

The purpose of the present paper is to explore time-dependent, fan reconnection models. In particular, we are interested in the question of whether fan solutions can produce fast ohmic dissipation, that is, whether they can release magnetic energy at a rate independent of the plasma resistivity η . The background to the problem is detailed in Sec. II where we introduce the governing magnetohydrodynamic (MHD) equations. In Sec. III the wave properties of the solution are discussed and it is shown that a Klein–Gordon equation governs the ideal “plane-wave” solution for the field disturbance. Section IV interprets this analysis in terms of the dynamic, planar solutions presented by previous authors.¹⁰ Finally, in Sec. V, we give a detailed discussion of the dynamic, three-dimensional merging problem and quantify the conditions under which fast ohmic release is possible.

II. TIME-DEPENDENT RECONNECTION ANALYSIS

A. Introduction

The basic idea of fan current reconnection is shown in Fig. 1. Curved field lines are washed into the reconnection region through the planes $x = \pm 1$. There is a global current sheet, localized over the plane $x = 0$, across which approaching field lines are cut and reconnected at the neutral point. Exact steady-state solutions of the fan current mechanism are already available.¹¹ What we develop here is a fully dynamic description.

B. Master equations

We assume that the plasma is governed by the incompressible, resistive MHD equations. An open geometry is assumed which allows the flow of mass and energy through the surfaces bounding the reconnection volume. Adopting nondimensional variables, in which fluid velocities are ex-

^{a)}Electronic mail: i.craig@waikato.ac.nz

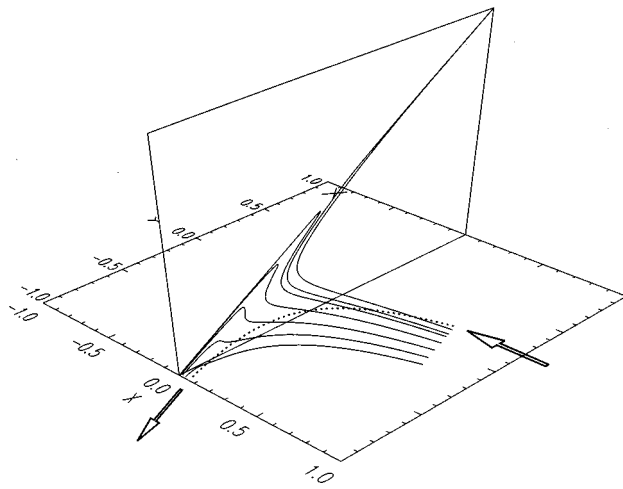


FIG. 1. A field line lying in the plane $y=z$ is advected across the spine for axisymmetric fan current reconnection. The arrows and dotted line shows the direction and motion of the plasma that carries the field across the spine. Parameters are $\eta=10^{-3}$, $\kappa=\beta=1/2$, $\alpha=1$, $Y(1)=Z(1)=0.05$.

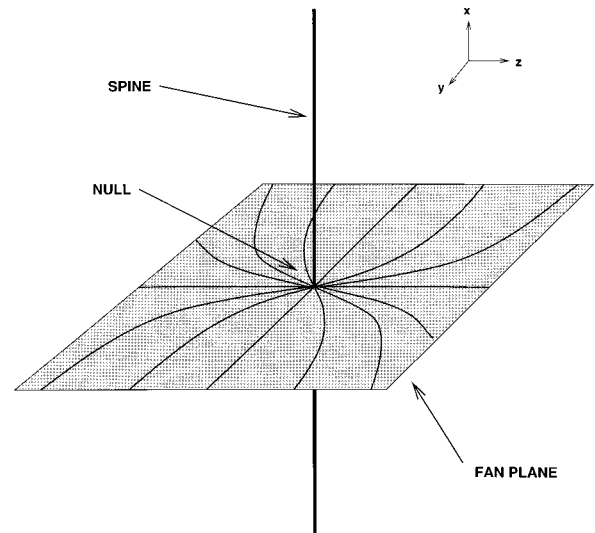


FIG. 2. Schematic spine and fan structure for an isolated X-point null.

pressed in units of the Alfvén speed at the boundary of the reconnection region, the momentum and induction equations can be written in the form

$$\frac{\partial \boldsymbol{\omega}}{\partial t} + (\mathbf{v} \cdot \nabla) \boldsymbol{\omega} - (\boldsymbol{\omega} \cdot \nabla) \mathbf{v} = (\mathbf{B} \cdot \nabla) \mathbf{J} - (\mathbf{J} \cdot \nabla) \mathbf{B}, \quad (1)$$

$$\frac{\partial \mathbf{B}}{\partial t} + (\mathbf{v} \cdot \nabla) \mathbf{B} - (\mathbf{B} \cdot \nabla) \mathbf{v} = \eta \nabla^2 \mathbf{B}, \quad (2)$$

where we have normalized the plasma density to $\rho \equiv 1$. The current density and the vorticity are given by

$$\mathbf{J} = \nabla \times \mathbf{B}, \quad \boldsymbol{\omega} = \nabla \times \mathbf{v},$$

where the field and flow are constrained by

$$\nabla \cdot \mathbf{B} = 0, \quad \nabla \cdot \mathbf{v} = 0.$$

Note that we employ the ‘‘curled’’ form of the momentum equation. The plasma pressure may be recovered from the uncurled form of the momentum equation once \mathbf{B} and \mathbf{v} have been determined.

The system is conservative apart from the resistive energy losses of the plasma. The resistivity is assumed constant and uniform and in the present units η has the dimensions of an inverse Lundquist number. Since η is typically of order 10^{-12} , the ohmic dissipation rate over the reconnection region R , namely

$$W_\eta = \eta \int_R J^2 d^3 \mathbf{r} \equiv \eta \langle J^2 \rangle, \quad \langle \chi \rangle \equiv \int_R \chi d^3 \mathbf{r}, \quad (3)$$

is quite negligible unless the plasma contains strong localized currents. It follows that, if magnetic reconnection is to be significant as an energy conversion mechanism, then extremely large current densities must develop over small length scales to enhance the ohmic dissipation rate. Studies of the solar atmosphere, in fact, suggest that a ‘‘fast’’ reconnection mechanism is required to account for the explosive

energy release of the solar flare. Accordingly, fast reconnection solutions provide a central goal of magnetic reconnection theory.

C. Time-dependent fan current reconnection

To develop solutions we assume that the magnetic and velocity fields can be represented by the superposition of a steady global field $\mathbf{P}(\mathbf{r})$ and a transient disturbance field $\mathbf{Q}(\mathbf{r}, t)$. The simplest representation of $\mathbf{P}(\mathbf{r})$ —though by no means the only one—is provided by the three dimensional X-point form

$$\mathbf{P}(\mathbf{r}) = -x\hat{\mathbf{x}} + \kappa y\hat{\mathbf{y}} + (1 - \kappa)z\hat{\mathbf{z}}. \quad (4)$$

By taking $0 \leq \kappa \leq 1$ we maintain a special role for the x axis. In terms of the eigenstructure of the null, this field line forms the ‘‘spine’’ of the background field, that is the unique field line into the null. Separatrix field lines emerging from the null can—as illustrated in Fig. 2—be visualized as a ‘‘fan’’ in the plane $x=0$. The illustrated null is positive, since more field lines exit the null than enter it.¹²

As Craig and Fabling⁷ have emphasized, the form of the reconnection is determined by whether the fan or the spine is distorted by the disturbance field. In the analysis that follows we concentrate on fan reconnection in which current sheets develop in the fan plane. The disturbance field is represented by plane waves propagating along the spine axis and solutions are developed by setting

$$\mathbf{Q} = \mathbf{Q}(x, t), \quad \mathbf{Q} \cdot \hat{\mathbf{x}} = 0. \quad (5)$$

The influence of the disturbance field is most easily visualised in the case of a planar null ($\kappa=1$, say). As Fig. 3 illustrates, there are two special cases, depending on whether the background field is distorted in the plane of the null, or at right angles to it. In both cases the disturbance tends to localize in a narrow current layer ($x \approx 0$) overlying the neutral point. However, in contrast to the perpendicular waves, the planar disturbances drive reconnection—that is, they distort the separatrix plane $y=0$ of the background field. More gen-

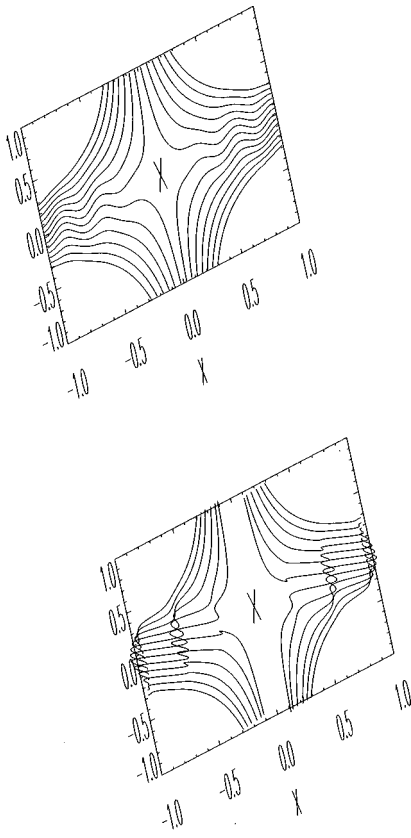


FIG. 3. Schematic showing the distinction between perpendicular (lower) and planar (upper) wave forms superposed on a two-dimensional X -point. If we assume the field disturbance is only in the y direction these two pictures correspond to $\kappa=0$ and $\kappa=1$, respectively.

erally, since perpendicular modes cannot be amplified by the background flow, it is only the planar modes that have the potential for fast reconnection.⁶ Although the distinction between planar and perpendicular disturbances no longer holds for three-dimensional nulls, we shall find that the orientation of the disturbance field to the background flow remains a key factor in determining the properties of the magnetic energy release.

Finally, we note that a second form of reconnection—in which the fan surface is distorted—can also be developed using the present formulation. The disturbance field has a form $\mathbf{Q} = Q(y, z, t)\hat{\mathbf{x}}$ and involves quasi-cylindrical currents aligned to the spine axis. Although the spine formulation leads to richer current structures, the magnetic energy in the disturbance field is typically many orders of magnitude weaker than the fan model.⁹ A brief discussion of spine current reconnection is given in Appendix B.

D. Fan reconnection equations

To construct fan current solutions we substitute the forms

$$\mathbf{v} = \alpha \mathbf{P}(\mathbf{r}) + V(x, t)\hat{\mathbf{y}} + W(x, t)\hat{\mathbf{z}}, \quad (6)$$

$$\mathbf{B} = \beta \mathbf{P}(\mathbf{r}) + Y(x, t)\hat{\mathbf{y}} + Z(x, t)\hat{\mathbf{z}}, \quad (7)$$

with α and β positive constants, into the momentum and induction equations. The sign of β is arbitrary but α must be positive to maintain the sign of the null. The evolution equations can be written in the form

$$V_t = \alpha(xV_x - \kappa V) - \beta(xY_x - \kappa Y) + f_V(t), \quad (8)$$

$$Y_t = \alpha(xY_x + \kappa Y) - \beta(xV_x + \kappa V) + \eta Y_{xx}, \quad (9)$$

$$W_t = \alpha(xW_x - (1 - \kappa)W) - \beta(xZ_x - (1 - \kappa)Z) + f_W(t), \quad (10)$$

$$Z_t = \alpha(xZ_x + (1 - \kappa)Z) - \beta(xW_x + (1 - \kappa)W) + \eta Z_{xx}, \quad (11)$$

where f_V and f_W are arbitrary functions of time. We note that the y components of \mathbf{Q} completely decouple from the z components. In fact we need only consider the $Y - V$ pair since the expressions for $Z - W$ follow from the simple replacements $\kappa \rightarrow (1 - \kappa)$, $Y \rightarrow Z$, $V \rightarrow W$. In addition, we observe that since the variable change $x \rightarrow \eta^{1/2}x$ eliminates the explicit η dependence of this system, there appears to be a natural small length scale in the x direction. We shall see later that $\eta^{1/2}$ determines the scaling of the current layer overlying the neutral point.

E. The plasma pressure

The plasma pressure can be deduced from the uncurled form of the momentum equation,

$$p(\mathbf{r}, t) = p_0(t) - \frac{1}{2}(\alpha^2 P^2 + Q^2) - \beta(\kappa y Y + (1 - \kappa)z Z) - y f_V(t) - z f_W(t), \quad (12)$$

where $Q^2 = Y^2 + Z^2$ determines the magnetic pressure of the disturbance field. This expression immediately brings out the problem with steady-state, flux pile-up solutions, in which Q^2 increases indefinitely as $\eta \rightarrow 0$.^{11,13-15} Since p_0 must scale as $Q^2/2$ to maintain positive pressures in the reconnection region, we see that unbounded pressures are required in the limit of small η .

More physically, we can identify p_0 with the magnitude of external hydromagnetic pressures which sustain the background flows that stretch and amplify the disturbance field. The fact that the pressure must be bounded in any realistic plasma shows that the flux pile-up solutions eventually saturate (at some sufficiently small resistivity) in any viable model of the reconnection process.⁹ This point is discussed further in Sec. VI.

In the analysis that follows we assume that all the disturbance fields are odd in order to maintain the null point of the field and stagnation point of the flow at the origin. In this case we must take $f_V(t) = f_W(t) = 0$.

F. The global energy balance

In studying fast reconnection solutions we are primarily interested in quantifying the ohmic losses for realistic values of the plasma resistivity. In an open geometry however, there may be a flux of mass and energy through the boundaries of the reconnection region R —which we take to be the unit cube—that contributes to the decay of the disturbance field.

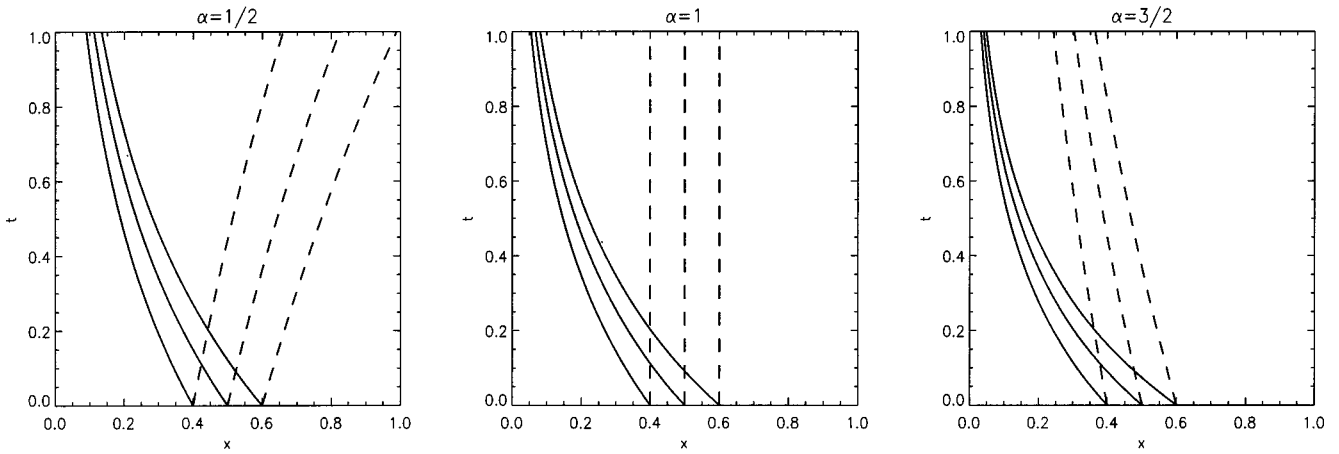


FIG. 4. Characteristics for the propagation of the field disturbance [Eq. (16)]. There are, in general, two wave speeds with characteristics C^+ (solid line) and C^- (dashed line). For all three values of α we take $\beta=1$. Only in the case $\alpha>\beta$ do both wave profiles localize.

These contributions must be quantified if we are to avoid confusing the field decay with the global ohmic losses.

The global energy losses are defined by the time derivative of $\langle B^2 + v^2 \rangle / 2$. For our purposes it is sufficient to consider only contributions from the y components of the disturbance field. The analysis of Appendix A gives

$$\begin{aligned} \dot{E} = & 4A_1(t) - \frac{1}{2}\alpha(1 - \kappa)\langle Y^2 + V^2 \rangle + \frac{1}{2}\alpha\kappa\langle Y^2 \rangle - \frac{3}{2}\alpha\kappa\langle V^2 \rangle \\ & + \beta\langle VY \rangle - \eta\langle J^2 \rangle, \end{aligned} \tag{13}$$

where $A_1(t) = \alpha(V_1^2 + Y_1^2) - 2\beta V_1 Y_1$.

It is clear that only the last term in Eq. (13) is associated with the ohmic losses of the plasma: If α or β is nonzero then other mechanisms can affect the energy contained in the reconnection volume R . For example, the term $A_1(t)$ reflects the energy flux at the inflow boundaries ($|x|=1$). Even if α vanishes, energy can still escape via shear waves propagating along the background magnetic-field lines—hence the term $\beta\langle VY \rangle$ in the energy equation.⁶

When a background stagnation point flow is present ($\alpha > 0$) the plasma can also advect energy out of the volume, as reflected by the second term in Eq. (13). The third term—namely $\frac{1}{2}\alpha\kappa\langle Y^2 \rangle$ —describes the energy increase due to the stretching of the disturbance field by the background flow. The fourth term quantifies the nonlinear interaction between the background and disturbance flows.

III. WAVE PROPERTIES OF THE SOLUTION

A. The wave equation

Suppose some long wavelength disturbance field $\mathbf{Q}(x, t)$ is superposed on the background X -point. The plasma resistivity can have little physical effect until the disturbance has localized to some small length scale determined by η . This localization phase is governed by the advection of the disturbance field and—as planar studies confirm⁶—it is the buildup in the wave amplitude that governs the strength of the nascent current layer.

The advection problem is much simplified by introducing the co-moving frame

$$\tau = t, \quad \xi = xe^{\alpha t}. \tag{14}$$

It follows, on eliminating V from Eq. (9), that Y evolves according to the Klein–Gordon equation

$$Y_{\tau\tau} = \beta^2 Y_{\chi\chi} + \kappa^2(\alpha^2 - \beta^2)Y, \quad \chi = \ln \xi, \quad \eta = 0. \tag{15}$$

Indeed it can be shown that Eq. (15) holds for any linear combination of Y and V .

The Klein–Gordon equation implies that the fan reconnection problem can be likened to the one dimensional, forced oscillations of an elastic medium. Specifically, Equation (15) derives by taking the extremum of the Lagrange density,

$$\mathcal{L}(Y, Y_\tau, Y_\chi) = \frac{1}{2}(Y_\tau^2 - \beta^2 Y_\chi^2 - \kappa^2(\alpha^2 - \beta^2)Y^2).$$

The first two terms represent the exchange of kinetic and potential energy densities during the oscillation while the final term governs the external driving of the wave. This driving is determined, not only by the magnitude ($\alpha^2 - \beta^2$), but also by the isotropy κ of the background field. Note also that when β vanishes no restoring force is provided by the medium. For the magnetic reconnection problem this limit corresponds to the absence of a background potential field: Straight field lines are driven together by the external flow ($\alpha > 0$), and no restoring force is available to limit the compression. This is an artefact of the open flow, incompressible formulation. In reality, the plasma pressure accumulated in the current sheet must eventually feed back on the “external” hydromagnetic forces that drive the merging.⁹

B. Characteristics of the flow

Returning to the Klein–Gordon Eq. (15), we note that the solution has two characteristics, namely, $C^\pm = \chi \pm \beta\tau$, or in real space

$$C^+ = xe^{-(\alpha+\beta)t}, \quad C^- = xe^{-(\alpha-\beta)t}. \tag{16}$$

As summarized in Fig. 4, an arbitrary initial wave envelope centred about the point $x = x_0$ (say), splits into two components. The component associated with the C^+ characteristic rapidly localizes, but the other only localizes if $\alpha > \beta$. In the special case $\alpha = \beta$ the solution reduces to an inward propa-

gating pulse plus a standing wave component. For $\alpha < \beta$ the C^- pulse broadens and propagates away from the origin. The key point is that only inward moving waves localize in real space, driving increasingly large currents as they approach the plane $x=0$.

The wave amplitude can also increase as the pulse localizes. If the tension term $\beta^2 Y_{\chi\chi}$ is small enough to be neglected, then

$$Y(\xi, \tau) \rightarrow Y_0(\xi) e^{\kappa(\alpha^2 - \beta^2)^{1/2} \tau}.$$

Since the tension term provides an extra energy loss mode for the plasma, we deduce that the localization criterion $\alpha > \beta$ provides a necessary condition for growth.

C. Fourier representation of the wave solution

The previous considerations are reinforced by taking a Fourier transform in χ -space. The Klein–Gordon equation reduces to

$$\bar{Y}_{\tau\tau} = (\kappa^2(\alpha^2 - \beta^2) - \beta^2 k^2) \bar{Y}, \tag{17}$$

$$\bar{Y}(\chi, \tau) = \int_{-\infty}^{\infty} \exp(-ik\chi) Y(k, \tau) dk,$$

which yields the formal solution

$$Y(\chi, \tau) = \frac{1}{2\pi} \int_{-\infty}^{\infty} dk A_{\pm}(k) \exp(ik\chi) \exp(\pm \nu(k) \tau) \tag{18}$$

where

$$\nu(k) = \sqrt{\alpha^2 \kappa^2 - \beta^2(\kappa^2 + k^2)}.$$

Growth requires $\Re(\nu) > 0$ and a necessary condition is clearly that $\alpha\kappa \neq 0$. By choosing $\kappa=0$ the flow becomes planar, but oriented at right angles to the direction of the disturbance field. In this case the disturbance field cannot be stretched and magnified by the background flow [see Eq. (19) below].

Growth also depends on the spectral character of the initial disturbance. Although the wave solution is formally defined on a noncompact space domain, namely $0 < |\chi| < \infty$, the solution is actually restricted to the space interval $\Delta x \leq x \leq 1$ where Δx is the width of the current sheet. A global initial disturbance requires $k |\ln \Delta x| \approx 1$. The scaling of the resistive layer (see Secs. IV B and V B) implies that $k \ll 1$ and so the conditions $\alpha > \beta$, $\kappa > 0$ are effectively sufficient for growth.

Finally, we mention two special cases in which wave packet solutions are possible. When $\beta=0$, corresponding to the merging of straight field lines driven together by the background flow, we obtain the wave solution

$$Y(x, t) = e^{\kappa\alpha t} Y_0(\xi), \quad \xi = xe^{\alpha t}. \tag{19}$$

Another simple case is provided by taking $\alpha = \beta$. The wave speeds are $\pm \beta$ in χ -space corresponding to the real space solution

$$Y(x, t) = G(xe^{2\alpha t}) + H(x). \tag{20}$$

TABLE I. Categorization of the known planar time-dependent models in terms of the notation of Sec. II.

Planar models ($\kappa=1$)	Background flow $\alpha \neq 0$	Background field $\beta \neq 0$	Planar components	Nonplanar components
Clark	✓	x	$V=0$	x
Bulanov <i>et al.</i>	x	✓	✓	x
Henton	✓	✓	✓	x
Craig and McClymont	✓	✓	✓	✓

We recover a stationary component plus a wave propagating inwards at the speed $2\alpha x$. Again we see that localization of the wave is a necessary but not sufficient condition for growth in the solution.

IV. SPECIAL CASE SOLUTIONS

A. Introduction

Many of the limiting cases of Eqs. (8) and (9) have been discussed in the literature. All previous known dynamic solutions involve an ignorable coordinate, as summarized in Table I. Our present purpose is to show how the fan current analysis incorporates these solutions—and can be used to predict scaling laws and ohmic dissipation rates for all planar models. A detailed analysis of the three-dimensional resistive system is given in Sec. V.

B. Annihilation of straight field lines

As already mentioned, the limit $\beta=0$ corresponds to pure magnetic annihilation involving the merging of straight field lines. With $V=\beta=0$ the magnetic and velocity fields have the components

$$\mathbf{B} = (0, Y(x, t), 0), \quad \mathbf{v} = \alpha(-x, \kappa y, (1 - \kappa)z). \tag{21}$$

The Clark¹⁶ solution corresponds to the planar flow field $\kappa = 1$. Clark derives exact solutions and demonstrates, by means of concrete examples, the fast nature of the dissipation. Specifically, there is an initial phase in which the field advects into a narrow current layer overlying the neutral point, followed by a rapid ohmic dissipation phase in which the field is resistively annihilated.

The essence of the Clark result can be obtained by invoking the wave solution (19). This solution breaks down when the wave has localized sufficiently for resistive diffusion to become important. In the co-moving (ξ, τ) frame, the wave solution $Y = e^{\kappa\alpha\tau} Y_0(\xi)$ breaks down when $|\eta e^{2\alpha\tau} Y_{\xi\xi}| \approx |Y_{\tau\tau}|$. It follows that the wave solution remains valid for times less than the localization time

$$T \approx \frac{1}{2\alpha} \ln \left(\frac{\alpha\kappa}{\eta} \right). \tag{22}$$

When $t \approx T$ the wave has collapsed to the length scale $x \equiv \Delta x \approx \eta^{1/2}$ corresponding to the field buildup $Y \sim \eta^{-\kappa/2}$ and the current density $J \sim \eta^{-(1+\kappa)/2}$. The ohmic dissipation rate scales as

$$W_{\eta} \approx \eta J^2 \Delta x \sim \eta^{1/2-\kappa}, \tag{23}$$

and so any solution with $\kappa \geq 1/2$ is fast. The flux pile-up in the solution is reflected however, by the scaling of the plasma pressure

$$p_0 \sim \frac{1}{2} Y^2 \sim \eta^{-\kappa}. \tag{24}$$

We see that the ‘‘super fast’’ annihilation of the Clark solution ($\kappa = 1$) leads to the most severe pressure dependence. It appears that the $\kappa = 1/2$ axisymmetric solution allows the best compromise between achieving a weak pressure buildup and a fast annihilation rate. Note that the slow Sweet–Parker rate, namely $W_\eta \sim \eta^{1/2}$, is obtained when $\kappa = 0$. In this case the field is directed normal to the plane of the velocity field $\mathbf{v} = \alpha(-x, 0, z)$, and there is no flux pile-up.

C. Undriven shear flow reconnection

Suppose there is no background flow to drive the merging. Then $\alpha = 0$ and the magnetic and velocity fields are given by

$$\mathbf{B} = (-\beta x, \beta \kappa y + Y(x, t), \beta(1 - \kappa)z), \quad \mathbf{v} = (0, V(x, t), 0). \tag{25}$$

The case $\kappa = 1$ has been analyzed by Bulanov *et al.*¹⁰ and represents the propagation of shear wave disturbances in the plane of the background X-point field (see also Craig and Rickard¹⁷). More recently, Craig and McClymont⁶ have analyzed the time development of (nonreconnective) displacements perpendicular to the plane of the X-point. Either way, since the solution for an isolated Fourier mode is given by

$$Y_F(x, t) = e^{\nu t \pm ik(\ln x + \alpha t)}, \quad \nu(k) = \sqrt{\alpha^2 \kappa^2 - \beta^2(\kappa^2 + k^2)}, \tag{26}$$

we see that ν is purely imaginary for $\alpha = 0$. This precludes the growth of any Fourier component, independent of κ . The absence of flux pile-up, when coupled to the $\eta^{1/2}$ scaling of the current layer, implies that the dissipation rate must follow the slow Sweet–Parker scaling $W_\eta \sim \eta^{1/2}$ (see Craig and McClymont⁶ for an exact analysis).

There is, however, a caveat to the interpretation of these results. Both Bulanov *et al.* and Craig and McClymont demonstrate that the magnetic field actually decays rapidly, on a $|\ln \eta|$ time scale, rather than at the slow rate predicted above. The reason is apparent from the global energy balance (13),

$$\dot{E} = \beta \langle VY \rangle - \eta \langle J^2 \rangle.$$

We see from the $\beta \langle VY \rangle$ term that energy can be carried out of the reconnection region by shear waves propagating along the background magnetic field. The energy loss time scale is then determined by the time it takes for shear Alfvén waves, propagating from the boundary of the reconnection region, to approach the edge of the diffusion layer⁶ $x \approx \eta^{1/2}$. It is these Alfvénic losses, rather than the weak resistive losses, that dominate the decay of the disturbance field.

D. Driven shear flow reconnection

Fast reconnection becomes a possibility when strong external flows are available to drive the merging. The driven planar merging problem has been analysed by Henton¹⁸ ($\kappa = 1$) and Craig and McClymont⁶ and we shall give only a

summary discussion here. Although the problem is now more complicated than the driven annihilation of straight field lines—wave modes are present due to the curvature of the magnetic-field lines—the merging can be described in broadly similar terms. In particular, it can be shown that the conditions $\kappa \geq 1/2$, $\alpha > \beta$, remain sufficient for fast dissipation. Rather than go through this argument, which mimics that of Sec. IV B, we now present a detailed analysis of the three-dimensional merging problem.

V. THREE-DIMENSIONAL FAN RECONNECTION SOLUTIONS

A. Introduction

The problem is to determine the time-dependent components of the magnetic and velocity fields

$$\begin{aligned} \mathbf{B} &= (-\beta x, \beta \kappa y + Y(x, t), \beta(1 - \kappa)z), \\ \mathbf{v} &= (-\alpha x, \alpha \kappa y + V(x, t), \alpha(1 - \kappa)z), \end{aligned} \tag{27}$$

given some long wavelength initial disturbance. Although the evolution Eqs. (8) and (9) for the disturbance fields are quite complicated, we can make some analytic progress by considering only the initial field evolution. Indeed, we expect the wave properties of the disturbance field to determine the strength of the nascent current sheet and the character of the reconnective energy release.

To date the only analytic results for three-dimensional fan reconnection have been derived for the case of steady-state merging⁷ for which $V = \beta Y / \alpha$. However, the fact that the fan equations must be able to reproduce the steady-state limit suggests introducing

$$F(x, t) = V(x, t) - \frac{\beta}{\alpha} Y(x, t), \tag{28}$$

to measure departures from the steady-state solution.

Consider, for instance, an initial global disturbance of the magnetic field, $Y(x, 0) = Y_0(x)$ with $V(x, 0) = V_0(x) = 0$. We have that $F = -\beta Y / \alpha$ initially, but, according to the steady-state limit, $F(x, t)$ should diminish as the velocity field builds up. We now investigate the evolution of $F(x, t)$ under the conditions of three dimensional $0 < \kappa < 1$, strongly driven merging $\alpha > \beta$.

B. The localization phase

Using Eq. (28), the momentum and induction Eqs. (8) and (9) yield

$$F_t - \alpha^+ x F_x = -\alpha^- \kappa F - \frac{\beta}{\alpha} \alpha^- (x Y_x + \kappa Y) - \frac{\beta}{\alpha} \eta Y_{xx}, \tag{29}$$

$$Y_t - \alpha^- x Y_x = \alpha^- \kappa Y - \beta(x F_x + \kappa F) + \eta Y_{xx} \tag{30}$$

where

$$\alpha^+ = \frac{\alpha^2 + \beta^2}{\alpha}, \quad \alpha^- = \frac{\alpha^2 - \beta^2}{\alpha}.$$

These forms already suggest that, for finite $\beta \leq \alpha$, $F(x, t)$ initially evolves on a faster time scale than $Y(x, t)$. In par-

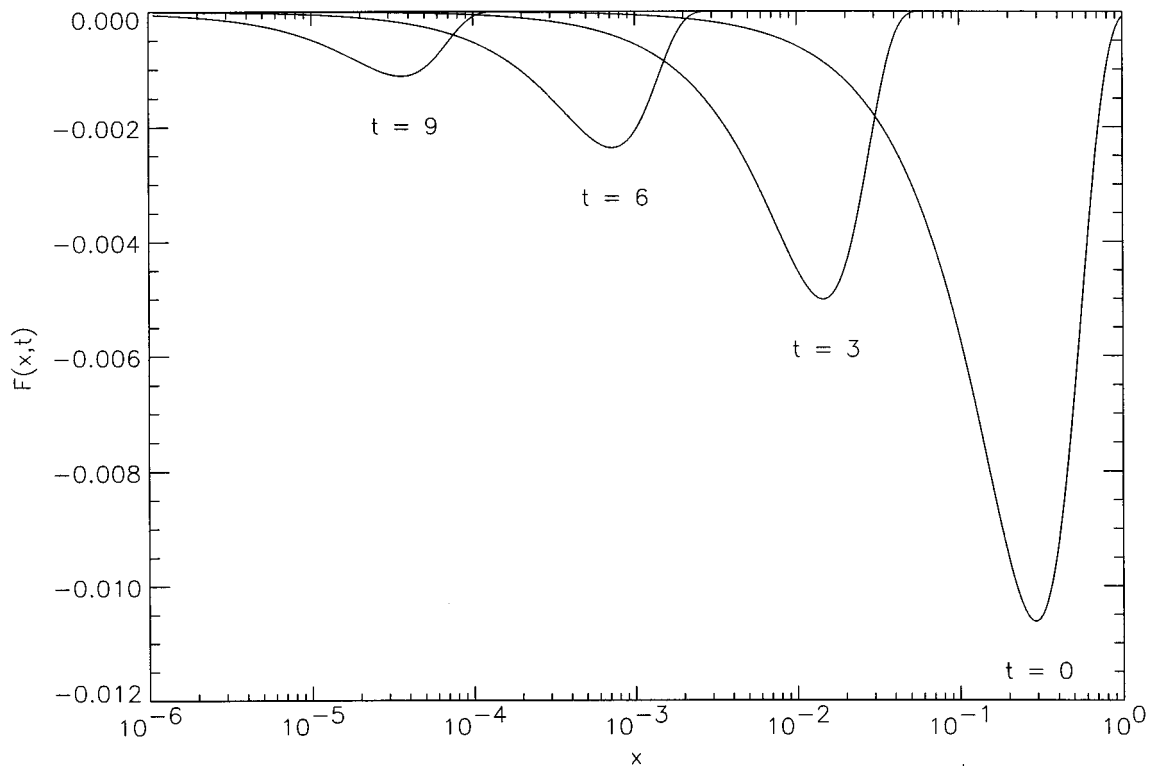


FIG. 5. The inward propagation of the degenerate flow profile. Because the momentum and induction equations decouple when $\beta=0$, the flow does not stop localizing when the $\eta^{1/2}$ length scale is attained. Parameters are $\alpha=1$, $\kappa=1/4$, and $\eta=10^{-2}$.

ticular, since α^- determines an inverse time scale for Y we see that the field localizes very slowly as $\beta \rightarrow \alpha$.

Suppose we examine the initial wave development under the assumption that α^- and α^+ define disparate time scales for the evolution. Consider the momentum Eq. (29). The diffusion term is negligible because the magnetic field has not yet localized; similarly, the term in $(xY_x + \kappa Y)$ is negligible whenever the product $\alpha^- \beta \rightarrow 0$. In this case

$$F(x,t) \approx F_0(\xi^+) e^{-\alpha^- \kappa t}, \quad \xi^+ = x e^{\alpha^+ t} \quad \alpha^- \beta \ll 1, \quad (31)$$

where $F_0(x) = -\beta Y_0(x)/\alpha$. Thus $F(x,t)$ rapidly localizes and weakly decays during the initial evolution.

The localization of $F(x,t)$, as illustrated in Fig. 5, is associated with the growth of the velocity field $V(x,t)$. That is, the magnetic and velocity fields approach the steady-state solution $V \approx \beta Y/\alpha$ in the outer region where $F \approx 0$. In fact it is natural to identify the growth of $V(x,t)$ with the fast characteristic C^+ in the general wave solution (Sec. III B). Under this interpretation it is the slower propagating C^- wave train that governs the amplification and localization of the magnetic field.

It follows that we can consider the magnetic-field advection in Eq. (9) under the assumption that the term in $(x F_x + \kappa F)$ is negligible. For either $F(x,t)$ has localized into the origin, or β is sufficiently small. Either way $Y(x,t)$ is given by

$$Y(x,t) \approx Y_0(\xi^-) e^{-\alpha^- \kappa t}, \quad \xi^- = x e^{\alpha^- t}, \quad (32)$$

a result which reflects the localization and growth of the field on the C^- characteristic. The growth will be arrested when $Y_t \approx \eta Y_{xx}$ close to the neutral point. Applying this condition to Eq. (32) implies the localization time

$$T \approx \frac{1}{2\alpha^-} \ln \left(\frac{\alpha^- \kappa}{\eta} \right), \quad (33)$$

provided that $\kappa \neq 0$. Upon back substitution of Eq. (33) into the ideal solution (32) we find that the current at the origin and hence the ohmic dissipation rate are given by

$$J \sim \eta^{-(1+\kappa)/2}, \quad W_\eta \sim \eta^{1/2-\kappa}. \quad (34)$$

Thus fast reconnection occurs only if $\kappa \geq 1/2$, in agreement with the planar analysis.

Before turning to the numerical confirmation of these results, we note one curious feature of the analysis. If we consider the case $\beta=0$ then Eqs. (8) and (9) decouple exactly. This is similar to the Clark limit, but suppose we now allow an initial disturbance flow profile $V_0(x) = V(x,0)$ to exist. The propagation of this shear flow is given by the replacement $F \rightarrow V, \alpha^+ = \alpha^- = \alpha$ in Eq. (31), specifically

$$V(x,t) = V_0(\xi) e^{-\alpha \kappa t}, \quad \xi = x e^{\alpha t}.$$

The interesting feature of this solution is that the inward advection of the wave does not stall! For finite κ the flow decays as it propagates inwards, but the decoupling from the induction equation means that the existence of a $\eta^{1/2}$ length scale cannot be conveyed to the flow. This anomaly persists in the numerics for small β but the disturbance is negligible energetically and does not effect the calculation of the diag-

nostics. In a more physical simulation, of course, this effect is overcome by specifying a nonzero plasma viscosity to damp out the strong vorticity that develops in the vicinity of the current sheet.

C. Numerical results

To explore the previous results we take $\alpha \equiv 1$ for all the numerical simulations and specify $0 < \beta < \alpha$ to ensure a strong localization of the field disturbance. We then carry out a series on small η runs with κ equal to 3/4, 1/2, and 1/4. The solution $Y-V$ for $\kappa = 1/4, 3/4$ can be thought of as the y and z components of the same disturbance field, since the planar and perpendicular terms are decoupled in the MHD equations.

We solve Eqs. (8) and (9) using a predictor-corrector method with an initial Gaussian-like field distribution with no disturbance flow component. This disturbance is “topological” since it distorts the spine of the background field: Therefore reconnection is required to ensure the recovery of the equilibrium state $V(x,t) = Y(x,t) = 0$.

As mentioned previously, we are faced with the problem of numerically modeling an open problem on a finite mesh. However, the choice $\alpha > \beta$ vastly simplifies the problem at the outer boundaries. With this constraint, we can be certain that the disturbance field/flow is only propagating inwards and hence we may set $V(1,t) = Y(1,t) = 0$ without having to worry about unphysical currents developing at the inflow surface. We note that Henton¹⁸ also considers an initial configuration that comprises a finite disturbance flow. We will not repeat the numerics for this condition since Henton demonstrates that essentially identical scalings are obtained from both approaches.

We are interested predominantly in three results from the numerical simulations: The field localization time, the energy decay rate and the effect of ohmic dissipation. We calculate these diagnostics by associating the localization time T with the time of maximum current at the neutral point. Care must be taken when calculating the decay rate of the total energy since the global energy may initially rise. This is due solely to the stretching of the field lines by the background flow. The condition at $|x| = 1$ eliminates the possibility of disturbance energy being washed through the inflow boundary. Finally, we define the decay time T_D as the time taken from the peak energy to decay to 1% of its maximum value.

The localization times agree remarkably well with the theory as demonstrated in Fig. 6. Restricting our attention to the lower range of η (between 3×10^{-4} and 10^{-6}) we calculate best fit scalings for the localization time as a function of $|\log \eta|$. In the limit $\beta = 0$, the approximate scaling is exact but this case results in annihilation rather than reconnection. For positive values of β , the approximate scalings for T and the current maximum are accurate up to quite large β .

Given that the flux pile up scales in the correct manner, we assume a field dissipation time based on the reconnective time scale

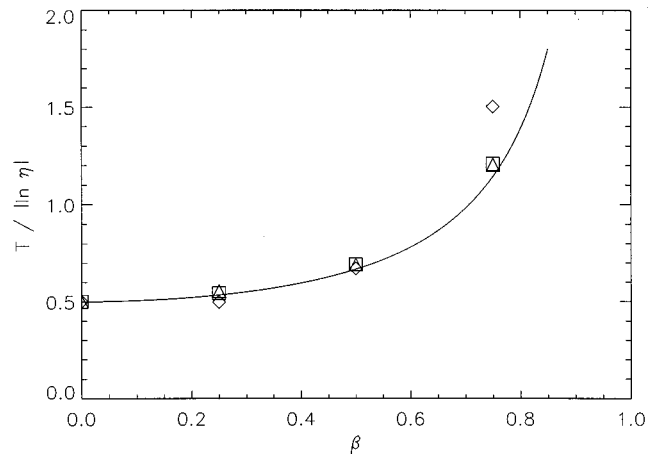


FIG. 6. Scaling of the localization time for different background field strengths. The different symbols represent $\kappa = 1/4$ (diamonds), $\kappa = 1/2$ (triangles), and $\kappa = 3/4$ (squares) while the solid line is the predicted scaling.

$$T_D \sim \frac{\langle B^2/2 \rangle}{W_\eta} \sim \eta^0. \tag{35}$$

Figure 7 confirms that the decay of the field and flow disturbances is almost independent of η over a very broad range of parameter space.

This result can also be checked by considering the total energy and the time integrated ohmic dissipation rate for the planar–nonplanar pairing $\kappa = 1/4, 3/4$. The details are shown in Fig. 8. We calculate the total energy dissipated by ohmic heating from the time when the current peaks. The expectation is that all nonreconnective disturbances will have exited the volume by this point (on the $|\ln \eta|$ time scale). The results support the theory very well. The energy dissipated by ohmic heating scales almost identically with the peak energy associated with the disturbance field.

Finally, we remark on the conditions required to achieve a significant total energy output from reconnection. Basically, it is only the component of the disturbance field that is aligned to the preferred direction of the background flow that

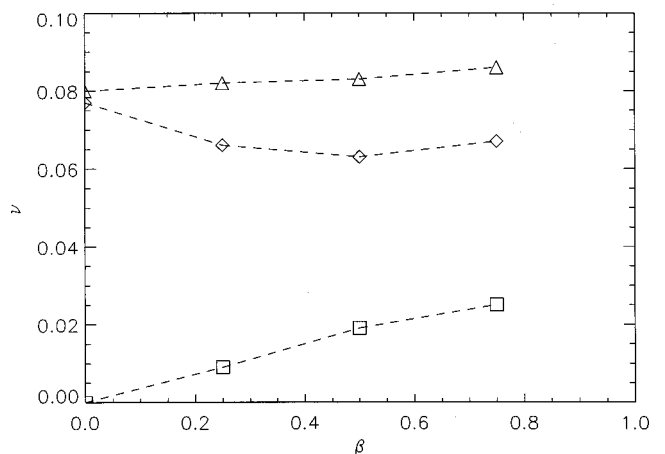


FIG. 7. Relationship between the energy decay time and η for different background potentials (assuming $T_D \sim \eta^0$). The different symbols represent $\kappa = 1/4$ (diamonds), $\kappa = 1/2$ (triangles), and $\kappa = 3/4$ (squares).

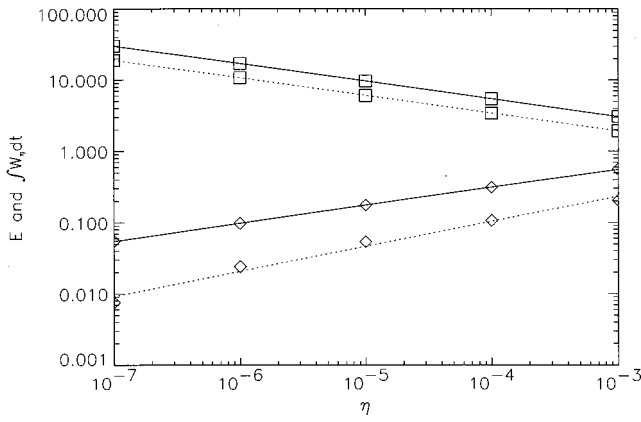


FIG. 8. Comparison of E after the field localization (solid line best fit) and the total energy dissipated through ohmic heating (dashed line best fit). The different symbols represent $\kappa=1/4$ (diamonds) and $\kappa=3/4$ (squares). In both cases there is no background magnetic field ($\beta=0$).

is “energetically” important. In other words, for a disturbance field in only the y direction we require $\kappa \geq 1/2$.

VI. CONCLUSIONS

The problem of dynamic, nonlinear, three-dimensional fan reconnection has been considered. We have shown that the problem can be understood as the superposition of finite amplitude, plane wave disturbances on background X -point equilibria. The resultant shear waves eventually localize into current sheets of width $\Delta x \sim \eta^{1/2}$ overlying the neutral point. The end result is magnetic reconnection and strongly enhanced rates of ohmic dissipation.

Yet fast reconnection can only occur if the waves are strongly driven by a global background flow ($\alpha > \beta$). In this case the localization of the disturbance field occurs over a $|\ln \eta|$ time scale and the topological energy of the disturbance is always rapidly dissipated, at a rate independent of the plasma resistivity. To release significant topological energy however, the wave field and the background flow must be suitably aligned. Thus a wave disturbance aligned to the y axis must be driven by a background flow field with $\kappa \geq 1/2$ if an energetically significant output is to be achieved.

It is interesting that the classical Sweet–Parker scaling, namely $W_\eta \sim \eta^{1/2}$, represents the slowest possible dissipation rate for the disturbance. This rate is accelerated according to the strength of the flux pile-up in the current layer. One difficulty for the present fast reconnection solutions is that, formally at least, the magnetic flux must increasingly pile-up as $\eta \rightarrow 0$. This can lead to huge plasma pressures in the reconnection region. A positive feature of the three-dimensional models, is that the scaling of the plasma pressure, viz. $p_0 \sim \eta^{-\kappa}$, is considerably less severe than for the planar models ($\kappa = 1$).

More physically, Craig *et al.*⁹ working in the context of steady-state, solar flare reconnection, consider the “saturated energy dissipation rate” obtained by bounding the plasma pressure to levels available in the solar atmosphere. Realistic pressures require that the amplitude of the disturbance field washed into the reconnection region be suitably limited. For $\kappa \approx 1/2$ fan current reconnection, it is found that both the

energy content of the disturbance field and the ohmic dissipation rate may be sufficient to account for modest flares, even at classical resistivity levels $\eta \approx 10^{-12}$. The fan reconnection mechanism becomes even more viable when it is remembered that micro-instabilities in the plasma lead to plausible enhancements of η by factors of 10^4 or more.¹ We have not considered the breakdown of the collisional resistivity, but the scaling of the current layer $\Delta x \approx \eta^{1/2}$ is certainly consistent with the breakdown of collisional conditions in the vicinity of the neutral point.

In this study we have only briefly mentioned the spine current reconnection mechanism. Unlike the current sheet structures of the fan model, spine reconnection involves time-dependent, tubular currents aligned to the spine axis. The radial extent of the current density (which scales as $\eta^{1/2}$) seems to preclude energy release comparable to the fan model, at least assuming realistic bounds on the plasma pressure. Despite this limitation, we believe it may be premature to reject spine reconnection as a viable energy conversion mechanism.

APPENDIX A: DERIVATION OF THE ENERGY EQUATION

Since the background field is an odd function of x , y , and z , only the disturbance field contributes to the global energy losses of the fluid. We can make a further simplification by exploiting the decoupling between the y and z components of the disturbance field and flow. Consider therefore the contribution

$$\dot{E} = \frac{1}{2} \langle (Y^2)_t + (V^2)_t \rangle. \quad (\text{A1})$$

Multiplying Eq. (9) through by Y gives

$$\frac{1}{2} (Y^2)_t = Y [\alpha (x Y_x + \kappa Y) - \beta (x V_x + \kappa V)] + \eta Y Y_{xx}. \quad (\text{A2})$$

On integration this yields

$$\begin{aligned} \frac{1}{2} \langle (Y^2)_t \rangle &= 4\alpha Y_1^2 + \alpha (\kappa - \frac{1}{2}) \langle Y^2 \rangle - \beta \langle x V_x Y \rangle - \beta \kappa \langle V Y \rangle \\ &\quad - \eta \langle (Y_x)^2 \rangle, \end{aligned} \quad (\text{A3})$$

where $Y_1 = Y(1, t)$ and we have assumed that the current is weak at the inflow boundaries. A similar calculation using the momentum equation implies

$$\frac{1}{2} \langle (V^2)_t \rangle = 4\alpha V_1^2 - \alpha (\kappa + \frac{1}{2}) \langle V^2 \rangle - \beta \langle x V Y_x - \kappa V Y \rangle. \quad (\text{A4})$$

Combining these two results yields Eq. (13).

APPENDIX B: SPINE CURRENT EQUATIONS

In the spine current formulation of the problem we take

$$\mathbf{v} = \alpha \mathbf{P}(\mathbf{r}) + U(y, z, t) \hat{\mathbf{x}}, \quad \mathbf{B} = \beta \mathbf{P}(\mathbf{r}) + X(y, z, t) \hat{\mathbf{x}}, \quad (\text{B1})$$

and the momentum and induction equations become

$$U_t = [1 - \mathcal{D}^\kappa] (\alpha U - \beta X) + f_U(t), \quad (\text{B2})$$

$$X_t = [1 + \mathcal{D}^\kappa] (\beta U - \alpha X) + \eta (X_{yy} + X_{zz}), \quad (\text{B3})$$

respectively where the differential operator \mathcal{D}^κ is given by

$$\mathcal{D}^\kappa = \kappa y \frac{\partial}{\partial y} + (1 - \kappa) z \frac{\partial}{\partial z}.$$

We dismissed this solution earlier on the grounds that the scalings were bound to be unfavorable given the steady-state analysis of Craig *et al.*⁹ Since the spine current solution is close to the threshold of being able to provide sufficient energy to describe a small flare (when we take into account the possible local enhancement of η), this form of reconnection should not be completely ignored.

¹E. N. Parker, *Cosmical Magnetic Fields* (Oxford University Press, London, 1979).

²D. Biskamp, Phys. Rev. Lett. **237**, 181 (1994).

³T. G. Forbes and E. R. Priest, Rev. Geophys. **25**, 1587 (1987).

⁴I. J. D. Craig and S. M. Henton, Astrophys. J. **450**, 280 (1995).

⁵R. B. Fabling and I. J. D. Craig, Phys. Plasmas **3**, 2243 (1996).

⁶I. J. D. Craig and A. N. McClymont, Astrophys. J. **481**, 996 (1997).

⁷I. J. D. Craig and R. B. Fabling, Astrophys. J. **462**, 969 (1996).

⁸E. R. Priest and V. S. Titov, Philos. Trans. R. Soc. London, Ser. A **354**, 2951 (1996).

⁹I. J. D. Craig, R. B. Fabling, and P. G. Watson, Astrophys. J. **485**, 383 (1997).

¹⁰S. V. Bulanov, S. G. Shasharina, and F. Pegoraro, Plasma Phys. Controlled Fusion **32**, 377 (1990).

¹¹I. J. D. Craig, R. B. Fabling, S. M. Henton, and G. J. Rickard, Astrophys. J. Lett. **455**, L197 (1995).

¹²E. R. Priest, J. Geophys. Res. **91**, 5579 (1986).

¹³B. U. O. Sonnerup and E. R. Priest, J. Plasma Phys. **14**, 283 (1975).

¹⁴P. G. Watson and I. J. D. Craig, Phys. Plasmas **4**, 101 (1997).

¹⁵G. W. Inverarity and E. R. Priest, Phys. Plasmas **3**, 3591 (1996).

¹⁶A. Clark, Phys. Fluids **7**, 1299 (1964).

¹⁷I. J. D. Craig and G. J. Rickard, Astron. Astrophys. **287**, 261 (1994).

¹⁸S. M. Henton, Ph.D. thesis, The University of Waikato, 1996.